



Surface analysis on anodized aluminum profiles with lubricating oils

Leonardo Corrêa Branco¹ Michel Domingues Silva² Polyana Alves Radi¹ Leonardo Henrique Fazan¹ Danieli Aparecida Pereira Reis^{1*} 

Abstract

The machining of aluminum requires less energy and enables high feed rates. Nevertheless, the material's elevated thermal expansion coefficient and elastic modulus pose challenges in achieving tight tolerances and contribute to a tendency for distortion. The 6060 alloy, extensively utilized in structural applications, consists of elements such as magnesium, silicon, iron, manganese, and copper, which form intermetallic phases that enhance its machinability, surpassing other aluminum alloys. During machining, most of the generated heat is absorbed by the workpiece, leading to deformation, handling difficulties, and shortened tool lifespan—issues that can be alleviated through the application of cutting fluids formulated with inactive sulfurized mineral oils. This research involved surface characterization through SEM, XRD, and tribological assessments using a pin-on-disk test on anodized 6060-T6 aluminum profiles, comparing two groups of specimens processed with and without cutting fluid. Additionally, an immersion test was performed on the specimens. The findings indicated that the specimens machined with cutting fluid demonstrated greater surface hardness and a reduced friction coefficient. SEM, EDS, and XRD analyses did not identify oxide formation or surface modifications in the specimens subjected to either immersion or machining with cutting fluid.

Keywords: Aluminum 6060-T6; Anodization; Cutting fluid; Tribology.

1 Introduction

Lightweight, strong, durable, and infinitely recyclable, aluminum has been gaining market share and is being used for a wide range of applications [1-4]. The use of aluminum profiles in civil construction increases productivity and efficiency, reduces the number of welds and screws, and simplifies the assembly process [5]. The aluminum oxide layer, naturally formed through contact with atmospheric air or induced by the anodization process, consists of a porous outer layer and an inner barrier layer [6], thus enhancing corrosion resistance. This layer also serves a decorative purpose and can be pigmented during anodization [7].

The 6060-T6 alloy contains magnesium and silicon as its primary alloying elements, as indicated by the first digit [6]. The second digit (0) signifies that no modifications have been made to the original alloy. The final digits (60) identify the specific alloy within the group [8]. This is a heat-treatable alloy in which material strengthening is achieved through the precipitation of an intermetallic compound, Mg_2Si [9]. The alphanumeric code (T6) indicates that the material has been artificially aged, being solution-treated and aged at temperatures

above room temperature [8]. Other characteristics of this alloy include high ductility, greater corrosion resistance compared to other heat-treatable alloys, good weldability, excellent compatibility with the anodization process [10], and a melting point ranging between 600 and 650 °C [11]. However, its low melting point is a primary disadvantage for aluminum applications [9].

During the machining process, three mechanisms generate heat: plastic deformation of the chip, friction between the chip surface and the tool, and friction between the workpiece and the tool's working region [12]. Most of this thermal energy is dissipated into the workpiece [approximately 73%, a reference value for turning]. Although this value varies depending on the operation, it is a critical consideration due to aluminum's low melting point. Therefore, cooling the tool-workpiece-chip system is necessary and can be achieved using cutting fluids [13].

Cutting fluids are a class of solid, liquid, or gaseous compounds employed to enhance the machining process. They provide economic benefits [reducing energy consumption, tool wear, and cost per machined part] and/

¹Laboratório de Comportamento Mecânico dos Metais, Universidade Federal de São Paulo – UNIFESP, São José dos Campos, SP, Brasil.

²Prolind Alumínio, São José dos Campos, SP, Brasil.

*Corresponding author: danieli.reis@unifesp.br

Adresses: lcbranco@unifesp.br; michel.silva@prolind.com.br; polyana.radi@unifesp.br; leonardo.fazan@unifesp.br



or functional advantages [improving cutting performance]. Surface finish is also improved when cutting fluids are used. For aluminum, it is recommended to use cutting fluids based on inactive sulfurized mineral fatty oils [13]. However, chemical interactions between the cutting fluid components, the oxide layer on the surface, and the aluminum alloying elements may affect the final finish and part performance [13].

Thus, this study aims to evaluate the performance of sulfurized fatty acid-based cutting fluids and the final quality of parts using manufacturing processes already employed by companies [14]. In this context, the influence of the lubricant on the surface of anodized aluminum profiles during the cutting stage was assessed. To this end, two groups of samples were studied: one machined with cutting fluid and the other without it.

2 Materials and methods

This work is part of the ELO Project, an initiative by ABAL aimed at fostering interaction between companies and universities through the co-supervision of technical projects. The study was developed in partnership between Prolind Aluminum and the Federal University of São Paulo.

2.1 Specimen preparation

At the Prolind Aluminum plant, 10 specimens with a height of 45 mm were cut across the width of a commercial piece, using cutting fluid, and another 10 specimens were cut without cutting fluid, employing an Atlas electro-pneumatic circular saw. Figure 1 shows the specimens which they were taken to the laboratory and resized for analysis. For this purpose, they were secured in a Tramontina Series 3000 vice with a cloth pad and slowly cut using a manual hacksaw equipped with new Starrett Redstrip 24-tooth blades. After cutting, the specimens were labeled, individually packaged, and stored in a location protected from light and moisture until the analyses were conducted.

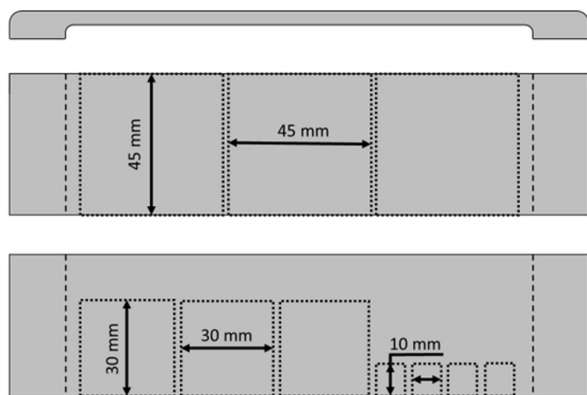


Figure 1. Schematic drawing of the cutting process performed on the pieces extracted from commercial 6060-T6 aluminum profiles.

2.2 Tribological study

The tribological study was based on the ASTM G133-95 standard [15], which defines the pin-on-disk test method. This standard was chosen for its wide acceptance and ability to simulate real-world wear conditions. The 100Cr6 steel sphere was chosen for tribological tests due to its standardized properties, aiming for consistent and reproducible results in evaluating anodized aluminium profiles. Its high hardness and wear resistance maintain a consistent contact interface, accelerating wear to highlight the effects of cutting fluid. While not directly used in aluminium rolling, 100Cr6 steel is relevant in industrial applications where aluminium contacts harder materials. The analysis was conducted using an Anton Paar TBR3 tribometer in pin-on-plate mode, employing a 100Cr6 steel sphere with a 6 mm diameter and specimens with dimensions of 30 x 30 mm. The tests were performed at a temperature of approximately 30 °C and a relative humidity of ~50%, using a linear reciprocating mode with a track length of 10 mm. In Table 1, the 18 measurements performed are presented, along with the detailed parameters and the sequence of test execution. At the end of each test, the sphere was rotated to a new area to ensure that wear from the previous test did not affect the results of the analysis. The specimens were labeled according to their preparation (CF – With Cutting Fluid and SF – Without Cutting Fluid), the analysis sequence, and the parameters of the tribological test (F: Load (N) and V: Speed in cm/s). The test parameters were selected based on an internal Anton Paar document, which recommended optimal settings, and the linear reciprocating mode, chosen to closely simulate the material's application.

2.3 Scanning Electron Microscopy

The scanning electron microscopy (SEM) analyses with energy-dispersive spectroscopy (EDS) were performed using the FEI Inspect S50 SEM model. The analyses were conducted on specimens cut with and without cutting fluid, with dimensions of 10 x 10 mm, using the secondary electron detection mode. Subsequently, EDS analysis was carried out.

2.4 X-ray diffraction

Specimens with dimensions of 10 x 10 mm were analyzed using XRD on a Rigaku, Ultima V, device with characteristic Cu-K α radiation. The parameters defined for the XRD analyses are listed in Table 2.

2.5 Specimen immersion test

An immersion test was conducted on the specimens in cutting fluid to evaluate potential surface alterations, simulating a scenario in which a specimen, after cutting, was

Table 1. Parameters and sequence of tribological tests

Specimen	Specimen Preparation	Test	Speed [cm/s]	Frequency [Hz]	Load [N]	Pressure [GPa]	Number of Cycles
CF 01	With oil	CF1F5V4	4	1.27	5	0.7	1000
CF 01	With oil	CF2F5V4	4	1.27	5	0.7	1000
CF 01	With oil	CF3F5V4	4	1.27	5	0.7	1000
CF 01	With oil	CF4F5V4	4	1.27	5	0.7	1000
CF 01	With oil	CF5F5V4	4	1.27	5	0.7	1000
CF 01	With oil	CF6F5V4	4	1.27	5	0.7	1000
SF 01	Without oil	SF1F5V4	4	1.27	5	0.7	1000
SF 01	Without oil	SF2F5V4	4	1.27	5	0.7	1000
SF 01	Without oil	SF3F5V4	4	1.27	5	0.7	1000
SF 01	Without oil	SF4F5V8	8	2.55	5	0.7	2000
SF 01	Without oil	SF5F5V8	8	2.55	5	0.7	2000
SF 01	Without oil	SF6F5V8	8	2.55	5	0.7	2000
SF 02	Without oil	SF1F10V8	8	2.55	10	0.88	2000
SF 02	Without oil	SF2F10V8	8	2.55	10	0.88	2000
SF 02	Without oil	SF3F10V8	8	2.55	10	0.88	2000
CF 02	With oil	CF1F10V8	8	2.55	10	0.88	2000
CF 02	With oil	CF2F10V8	8	2.55	10	0.88	2000
CF 02	With oil	CF3F10V8	8	2.55	10	0.88	2000

not properly cleaned and remained in contact with the fluid for several days. The test was performed on two specimens (cut with and without cutting fluid) with dimensions of 45 x 45 mm. These specimens were immersed in the cutting fluid for 37 days in a 250 mL beaker, using wooden fixtures to position the specimens so that half remained submerged in the fluid. Figure 2 presents the schematic drawing of the device used for the immersion test. Daily monitoring was carried out to check for any visual alterations on the surface of the specimens. To ensure consistent comparison, the positions of the beaker, lamp, and camera stand used for recording observations were carefully marked and maintained.

3 Results and discussions

Table 3 presents the tribological results obtained directly using the Anton Paar tribometer in accordance with the ASTM G133-95 standard [15]. In some specimens, the wear was smaller than the surface roughness of the specimen, making it impossible to measure the worn volume. Certain wear profiles exceeded the thickness of the anodized layer of the profile (15 μm), as illustrated in Figure 3.

The wear area and volume values were obtained using a Taylor Hobson - Surtronic S-128 profilometer, which was coupled with the Anton Paar tribometer. This integration allowed for measurements of the wear tracks generated during the tribological tests, enabling in-situ analysis of the wear scars without removing the specimens. After each test, the profilometer scanned the wear track, generating a surface profile. The software associated with the Anton Paar tribometer was then used to select the area of the wear track on the profile. Once selected, the software automatically calculated the wear rate based on the selected area and the test parameters. The software from Anton Paar

Table 2. Parameters of XRD analyses

Parameter	Value
Minimum Angle	30 °
Maximum Angle	85 °
Step	0.01 °
Speed	5 °/min
Voltage	40 kV
Current	30 mA
Divtt slit	10 mm
Div slit	1 mm
Sct slit	open
Ree slit	open
Fixed Angle	1.5 °

calculated the wear rate directly and eliminating manual calculations.

The lowest average friction coefficient values were observed for specimens cut with oil at the lowest speed (4 cm/s) and lowest load (5 N). Within this group, the analyses CF2F5V4 and CF5F5V4, which were conducted on a central portion of the specimen—further from the cutting fluid spray region—showed higher friction coefficients.

The lower friction values may be related to the residual presence of the cutting fluid [13]. However, specimens in the CF#2 group, cut with cutting fluid and tested at a load of 10 N and a speed of 8 cm/s, exhibited high friction coefficient values. This can be attributed to the increase in load and speed, where the fluid sprayed on the specimen surface was insufficient to ensure lubrication at the contact interface between the sphere and the specimen surface.

The average friction coefficient value was determined by extracting the positive peaks from the curve relating the friction coefficient to time in seconds, as presented in Figure 4. Curves with an average value of 0.11 showed minimal variation

Table 3. Results of the tribological study in pin-on-plate mode

Specimen	Specimen Preparation	Test	Maximum [μm]	Average [μm]	Wear Cross-Section Area [μm^2]	Volume [μm^3]
CF 01	With oil	CF1F5V4	0.18	0.11	-	-
CF 01	With oil	CF2F5V4	1.03	0.73	622	6.22×10^6
CF 01	With oil	CF3F5V4	0.16	0.11	-	-
CF 01	With oil	CF4F5V4	0.18	0.11	-	-
CF 01	With oil	CF5F5V4	1.02	0.72	-	-
CF 01	With oil	CF6F5V4	0.25	0.11	-	-
SF 01	Without oil	SF1F5V4	0.41	0.11	-	-
SF 01	Without oil	SF2F5V4	1.02	0.80	1.180	1.18×10^7
SF 01	Without oil	SF3F5V4	1.07	0.70	317	3.17×10^6
SF 01	Without oil	SF4F5V8	1.08	0.78	493	4.93×10^6
SF 01	Without oil	SF5F5V8	1.11	0.78	410	4.10×10^6
SF 01	Without oil	SF6F5V8	1.13	0.78	468	4.68×10^6
SF 02	Without oil	SF1F10V8	2.26	0.76	-	-
SF 02	Without oil	SF2F10V8	1.99	0.71	-	-
SF 02	Without oil	SF3F10V8	1.26	0.81	-	-
CF 02	With oil	CF1F10V8	2.11	0.73	-	-
CF 02	With oil	CF2F10V8	2.09	0.73	-	-
CF 02	With oil	CF3F10V8	2.07	0.72	-	-

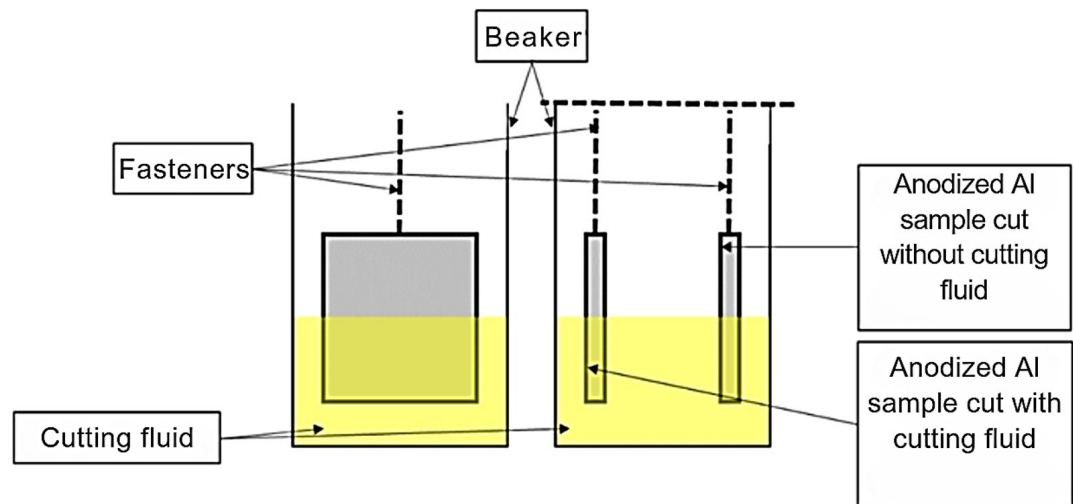


Figure 2. Schematic drawing of the device used for the immersion test of specimens in cutting fluid.

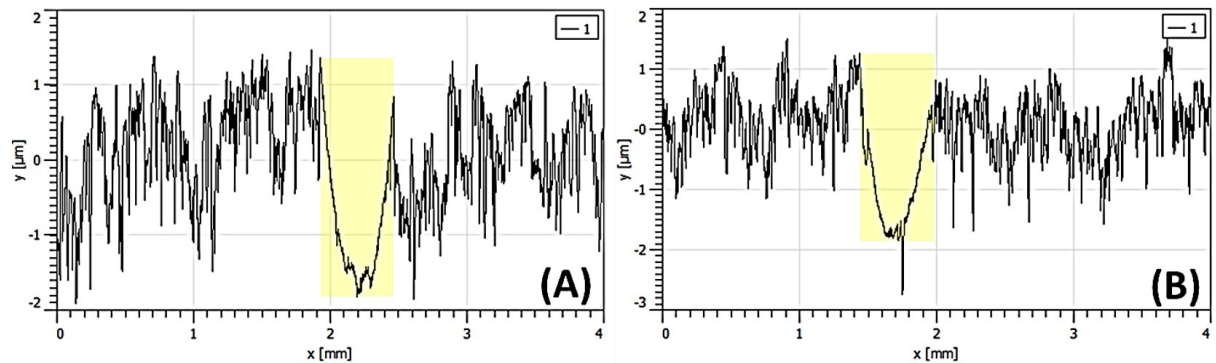


Figure 3. Wear profiles for specimens SO4F5V8 (A) and SO5F5V8 (B).

in the friction coefficient throughout the test (Figure 4A). In contrast, curves with an average friction coefficient close to 0.8 displayed a different behavior; as time progressed, the friction coefficient increased until stabilizing at values near 0.8, leading to the calculated average value (Figure 4B).

This behavior was attributed to the wear of the anodized layer, which allowed contact between the pin and the substrate. For specimens cut without cutting fluid, a high friction coefficient, ranging from 0.70 to 0.80, was observed as the dominant behavior. Only the SF1F5V4 test exhibited a lower friction coefficient value (0.11). This analysis was performed in a region near the circular saw cut, suggesting

that residual cutting fluid may have been present, contributing to the reduction in friction. Figure 5 shows the confirmation of cutting fluid contamination through EDS analysis.

The major compounds found in the specimens cut with and without oil were the same: aluminum, oxygen, carbon, and sulfur. The anodized layer consists of aluminum oxide (Al_2O_3), which indeed represents the highest concentration of compounds in the specimen. However, some alloying elements expected in the 6061-T6 alloy, such as magnesium and silicon, were not detected. Less intense peaks of sulfur and carbon were also observed. The carbon originates from the carbon tape used for grounding the specimen in the

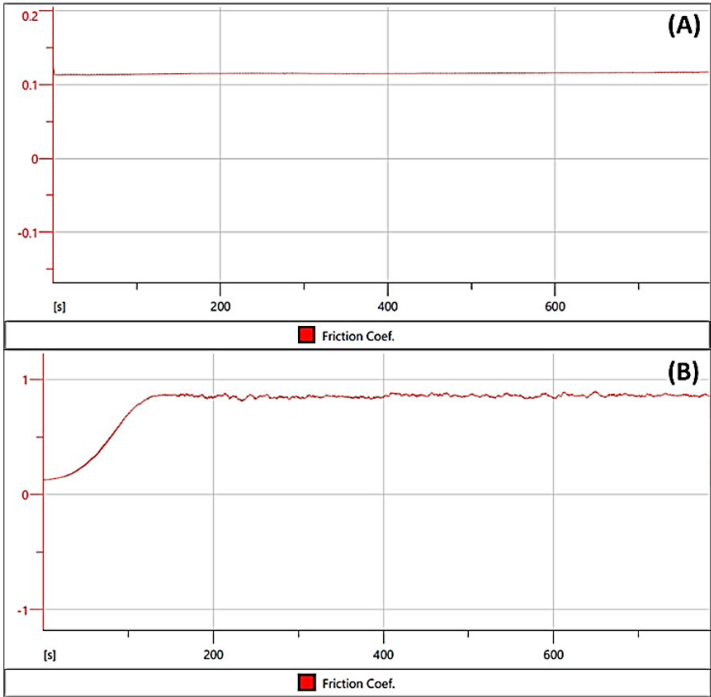


Figure 4. Example of friction coefficient curves showing the two observed behaviors, using tests CO1F5V4 (A) and SO3F5V4 (B) as references.

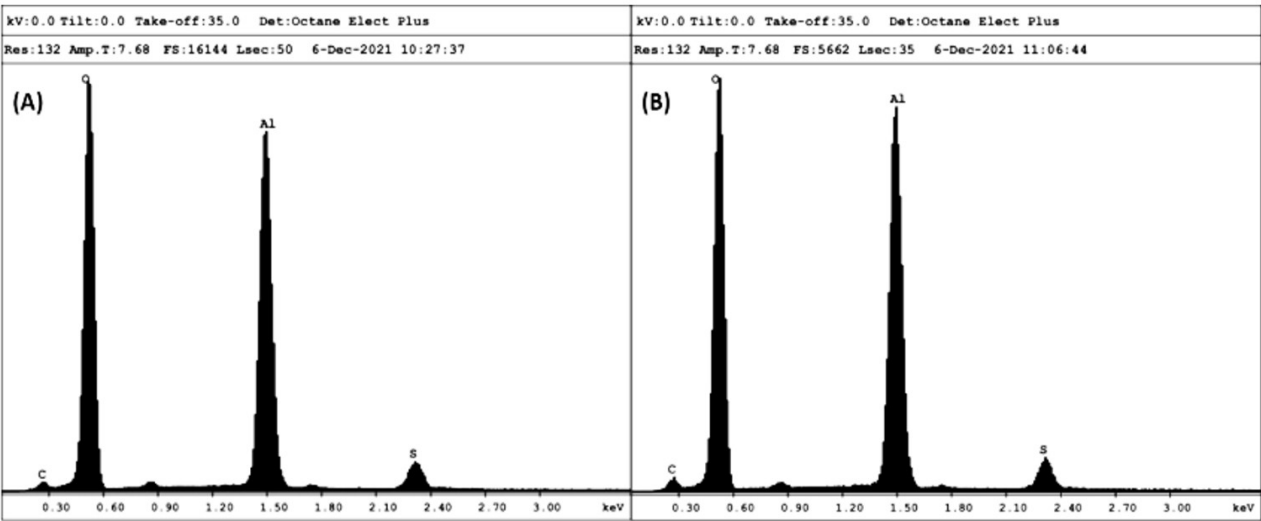


Figure 5. EDS spectrum for the specimen cut without oil (A) and the specimen cut with oil (B).

sample holder. The sulfur may derive from contamination by lubricating oil, which is composed of sulfurized fatty acids. Although the EDS technique provides a semi-quantitative

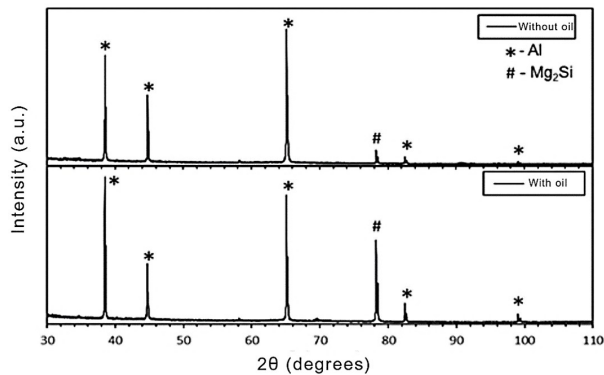


Figure 6. Diffractograms obtained for anodized aluminum specimens with a final angle of 110° and a fixed angle of 1.5° for specimens cut without and with lubricating oil.

analysis of the specimen's surface composition, it is important to note that more accurate and quantitative results depend on the flatness of the surface [16].

In the diffractograms shown in Figure 6, peaks corresponding to aluminum [17] and the Mg_2Si phase [18] can be observed. Magnesium and silicon are the alloying elements with the highest concentrations in the 6061 alloy, and the presence of the Mg_2Si phase increases the hardness of the alloy [9,19,20].

One of the specimens from the friction test exhibited a dark coloration within the wear track. This wear track was subsequently analyzed using EDS and SEM, as shown in Figure 7. The analyses suggest that the stain corresponds to steel deposition from the sphere of the end-effector onto the specimen, as evidenced by the presence of iron and carbon peaks.

The specimens were analyzed using SEM as shown in Figure 8. Three regions were examined: the cut region that remained immersed in oil (a), the central region at the interface between the immersed and non-immersed areas (b), and the final region that was not immersed (c). No

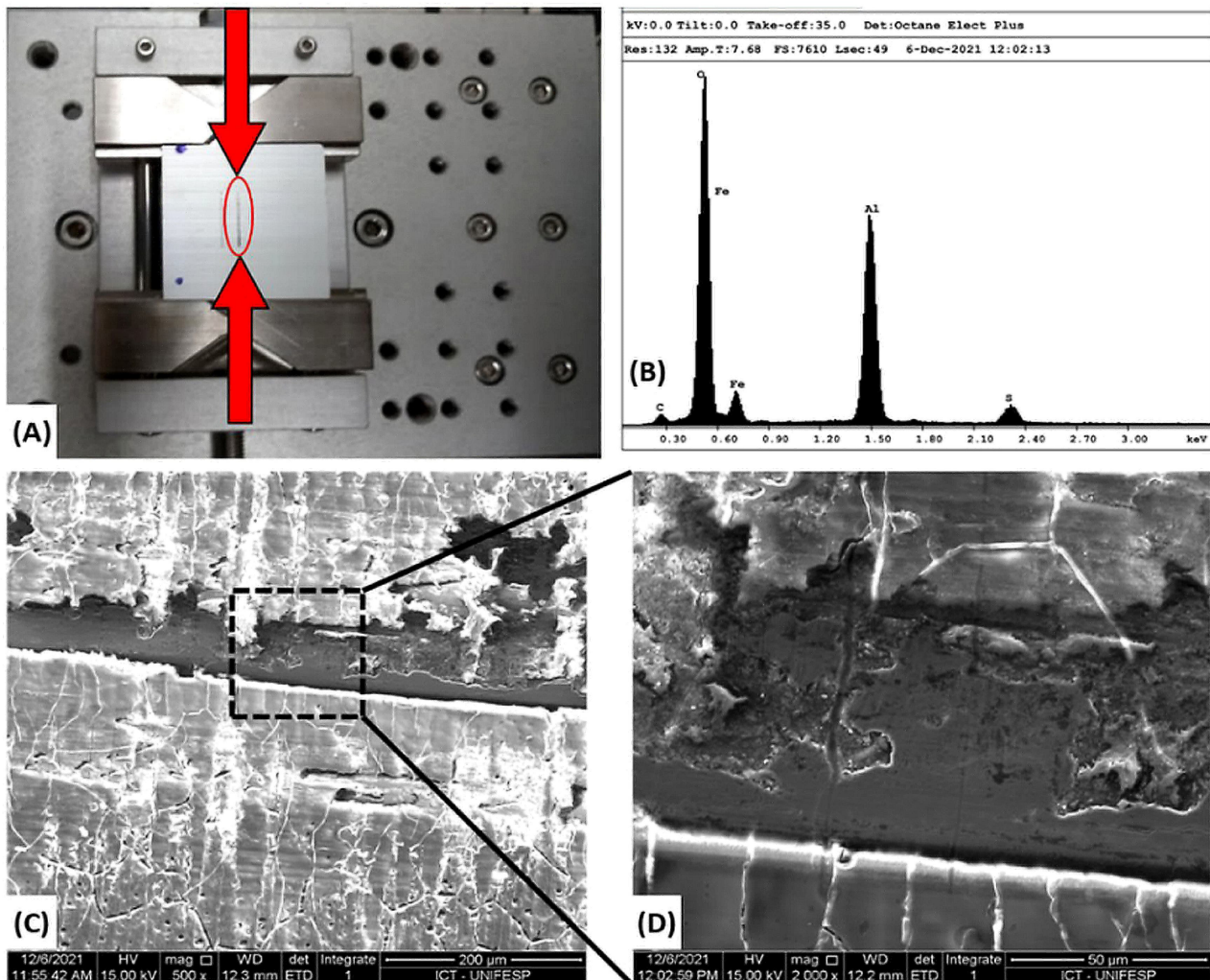


Figure 7. Analysis of the specimen that exhibited a dark stain after the friction test. (A) Photograph of the specimen mounted on the tribometer, highlighting the dark wear track; (B) EDS analysis within the track; (C) SEM image of the track region at 500x magnification; (D) SEM image of the track region at 2000x magnification.

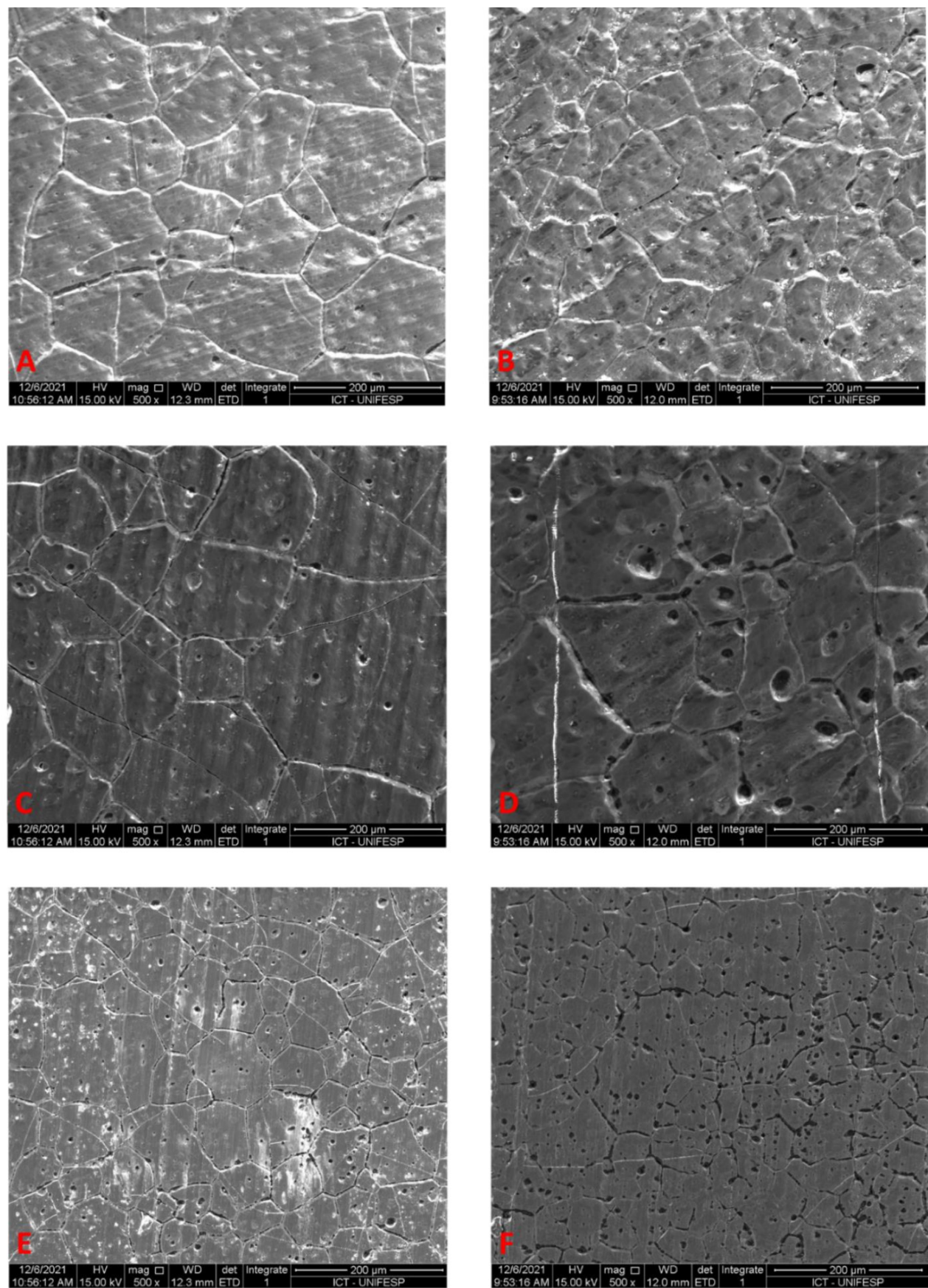


Figure 8. SEM micrographs of aluminum specimens cut with oil in the cut region (A), central region (C), and final region (E), and cut without fluid in the cut region (B), central region (D), and final region (F), at 3000x magnification.

significant differences were observed among the micrographs. Given the duration of the immersion period, no formation of oxides, surface stains, or defects affecting the visual appearance of the anodized layer, either macroscopically or microscopically, could be detected.

4 Conclusion

The use of cutting fluid raises concerns in some companies, as the material serves both structural and decorative purposes. In this study, no surface stains or macroscopic oxide formations were observed in either the cut specimens or those immersed in the cutting fluid for 37 days. SEM, EDS, and XRD analyses also did not reveal oxide formation on the specimen surfaces. The XRD analyses showed the presence of an Mg_2Si peak, which is responsible for the increased hardness of this alloy.

No significant differences were observed between the specimens cut with and without cutting fluid. Therefore, the

use of cutting fluid is recommended, as it extends the cutting tool's lifespan and prevents excessive heating, which could lead to deformations or dimensional errors in the final part.

For future work, it is recommended to evaluate the influence of temperature on the corrosion process [21], repeat analyses on specimens with a high degree of polishing [16], and use more precise characterization techniques for quantitative oxide detection, such as Raman Spectroscopy [22].

Acknowledgements

The authors express their gratitude to Prolind Aluminum and ABAL for the development of the ELO Project and their partnership throughout the execution of this work. Special thanks to Anton Paar, represented by Researcher Dr. Filipe Estevão, for providing access to the equipment in their showroom for the analyses, and to Researcher Dra. Renata Jesuina Takahashi for her support in the SEM and XRD analyses.

References

- 1 Rocha EG, Camarinha MGG, Reis DAP. Fractographic analysis of the AA 7075-T6 alloy subjected to fatigue in the RRA treatment condition and plasma nitride. *Revista Matéria* (Rio de Janeiro). 2023;28(1):1-10.
- 2 Pinho JSR, Campanelli LC, Reis DAP. Case study on the failure analysis of turbojet compressor blades. *Tecnologica em Metalurgia, Materiais e Mineração*. 2022;19:e2760.
- 3 da Silva GS, Camarinha MGG, Rocha LO, Barboza MJR, Martins GV, Reis DAP. Study of the influence of the RRA thermal treatment and plasma nitriding on corrosion behavior of 7075-T6 aluminum alloy. *Surface and Coatings Technology*. 2019;374:736-744.
- 4 Reis DAP, Couto AA, Domingues NI Jr, Hirschmann AC, Zepka S. de Moura C No. Effect of artificial aging on the mechanical properties of an aerospace aluminum alloy 2024. *Defect and Diffusion Forum*. 2012;326-328:193-8.
- 5 Mazzolani FM. Structural applications of aluminium in civil engineering. *Structural Engineering International. Journal of the International Association for Bridge and Structural Engineering*. 2016;16(4):280-285.
- 6 Yu X, Zhang G, Zhang Z, Wang Y. Research on corrosion resistance of anodized and sealed 6061 aluminum alloy in 3.5% sodium chloride solution. *International Journal of Electrochemical Science*. 2023;18(5):100092.
- 7 Fontana MG. *Corrosion engineering*. 3rd ed. New York: McGraw-Hill; 1986.
- 8 Associação Brasileira de Normas Técnicas. ABNT NBR 12609:2022 - Alumínio e suas ligas — Tratamento de superfície — Requisitos para anodização para fins arquitetônicos. Rio de Janeiro: ABNT; 2022.
- 9 Callister WDJ, Rethwisch GD. *Materials science and engineering: an introduction*. 10th ed. Hoboken: Wiley; 2018.
- 10 Reiso O. Extrusion of AlMgSi alloys. In: Nie JF, Morton AJ, Muddle BC, editors. *Proceedings of the 9th International Conference on Aluminium Alloys*; 2004; Brisbane, Australia. Australia: Institute of Materials Engineering Australasia Ltd.; 2004. p. 32-46.
- 11 Stojanovic B, Bukvic M, Epler I. Application of aluminum and aluminum alloys in engineering. *Applied Engineering Letters*. 2018;3(2):52-62.
- 12 Grzesik W. *Advanced machining processes of metallic materials: theory, modelling and applications*. Amsterdam: Elsevier; 2008.
- 13 Beladiya D, Chauhan IA. A study on principles of metal cutting: review. *International Journal of Advance Research and Innovation*. 2020;8(4):68-73.
- 14 Associação Brasileira do Alumínio. *Anuário Estatístico ABAL 2020*. São Paulo: ABAL; 2020.
- 15 ASTM INTERNATIONAL. ASTM G133-95: Standard test method for linearly reciprocating ball-on-flat sliding wear. West Conshohocken, PA: ASTM International, 1995
- 16 Girão AV, Caputo G, Ferro MC. Application of scanning electron microscopy–energy dispersive X-ray spectroscopy (SEM-EDS). *Comprehensive Analytical Chemistry*. 2017;75:153-168.

- 17 Zupanič F, Klemenc J, Steinacher M, Glodež S. Microstructure, mechanical properties and fatigue behaviour of a new high-strength aluminium alloy AA 6086. *Journal of Alloys and Compounds*. 2023;941:168976.
- 18 Tiwan, Ilman MN, Kusmono, Sehon. Microstructure and mechanical performance of dissimilar friction stir spot welded AA2024-O/AA6061-T6 sheets: effects of tool rotation speed and pin geometry. *International Journal of Lightweight Materials and Manufacture*. 2023;6(1):1-14.
- 19 Westbrook JH, Conrad H. The science of hardness testing and its research applications: Based on papers presented at a symposium of the American Society for Metals. Materials Park: American Society for Metals.
- 20 International Organization for Standardization. ISO 14577-4:2016 - Metallic materials — Instrumented indentation test for hardness and materials parameters — Part 4: Test method for metallic and non-metallic coatings. Geneva: ISO; 2016.
- 21 Associação Brasileira do Alumínio. Guia técnico do alumínio: extrusão. 4. ed. São Paulo: Editora Técnica Comunicação; 2008.
- 22 Orlando A, Franceschini F, Muscas C, Pidkova S, Bartoli M, Rovere M, et al. A comprehensive review on Raman spectroscopy applications. *Chemosensors (Basel, Switzerland)*. 2021;9(9):262.

Received: 27 Jan. 2025

Accepted: 11 Jun. 2025

Editor-in-charge:

Sabrina Arcaro 